Brillouin spectroscopy of surface modes in thin-film Si_3N_4 on GaAs

Pavel Zinin, Murli H. Manghnani, Sergei Tkachev, and Vahid Askarpour
School of Ocean and Earth Science and Technology, University of Hawaii, Honolulu, Hawaii

Odile Lefeuvre
Department of Materials, Oxford University, Oxford OX1 3PH, United Kingdom

Arthur Every
Department of Physics, University of the Witwatersrand, PO WITS 2050, South Africa
(Received 26 May 1998; revised manuscript received 8 March 1999)

We report here the determination, by surface Brillouin spectroscopy, of the dispersion relation of surface acoustic phonons localized at the free surface and interface of thin film Si_3N_4 on a GaAs substrate. A splitting in the dispersion curve representing velocity versus kh is observed experimentally. With increasing kh, starting from zero the Rayleigh mode of the substrate increases in velocity and then at a cut-off degenerates with the bulk mode continuum, and transforms into a pseudointerfacial wave. This mode propagates with attenuation along the layer-substrate interface, decaying exponentially with depth into the layer and leaking energy into the substrate. In the same range of kh beyond cutoff, a second mode appears that for large kh evolves into the Rayleigh wave of the film. The purpose of this paper is to demonstrate experimentally this splitting of the dispersion relation into two branches. This is the first reported observation, for a stiffening layer on a substrate, of a leaky interfacial wave, a type of mode that is of potential value in the interface characterization of thin supported transparent films. [S0163-1829(99)04928-0]

I. INTRODUCTION

The general features of surface acoustic wave (SAW) propagation in layered media have been widely researched.[1,2] Despite the extensive literature, there are only a few publications that deal with SAW's of stiffening layers, i.e. fast on slow systems (for which the shear wave speed of the layer is greater than that of the substrate). Recently there has been a surge of interest in such systems, since they provide a tool for the characterization of hard supported films of various kinds,[3] including traditional hard protective coatings[4,5] and topical materials such as fullerite and diamonds films.[6,7] It was shown in earlier works[1] that true SAW's (surface waves that do not leak energy into bulk) can propagate on stiffening layers only below the cut-off thickness at which the SAW slowness (inverse phase velocity) meets the transonic state, i.e., the limiting slowness of bulk modes parallel to the surface. The question about the existence of SAW's above cutoff was not clear until Bogy and Gracewski[8] found theoretically that leaky SAW's (LSAW) or pseudo-SAW's (PSAW) exist beyond the cutoff. PSAW above cutoff have been detected experimentally only recently by Pang *et al.*,[4] who used Brillouin spectroscopy to measure the dispersion of SAW on TiN films on steel. The complex dispersion curve (dispersion of SAW's velocity and attenuation) above cutoff has been investigated for an oxide film on aluminum.[9] Computer calculations carried out by Lefeuvre *et al.*[10] have revealed that for a very hard film as compared with the substrate, the surface wave above cutoff evolves into a leaky interfacial wave with increasing layer thickness. This is a mode that propagates along the interface between the layer and substrate, decaying exponentially with depth into the layer and leaking energy into the substrate, which causes it to attenuate with distance. This pseudointerfacial wave is localized quite strongly near the interface and promises to be useful for interface characterization. The purpose of this paper is to demonstrate experimentally that above cut-off the dispersion curve is, as it was predicted in,[10] split into two modes, the leaky interfacial wave and a Rayleigh mode localized near the free surface of the layer. To our knowledge, the present paper represents the first experimental observation of an interfacial wave for a stiffening layer system.

The technique we use for observing the interfacial wave is surface Brillouin spectroscopy, which in the case of a transparent film, is able to detect thermally induced dynamic rippling of the interface. Standard acoustic methods are not suited to the detection of these waves since for films much thicker than the wavelength, the interfacial waves do not extend as far as the free surface of the film, and so they cannot be excited or detected from the surface. The system we have studied is a Si_3N_4 film on GaAs; the film is transparent[11,12] and the substrate almost opaque (complex refraction index $n=4.21+i0.28$),[11] and the film is elastically much stiffer than GaAs. Most of the light scattering is therefore caused by phonons propagating at the Si_3N_4/GaAs interface. Moreover, since Si_3N_4 has a rather large value of refractive index ($n\sim 2$) the backscattering signal from the film surface (Si_3N_4/vacuum interface) is also moderately strong. Hence, we expect to be able to detect a contribution in the Brillouin spectrum also from surface scattering. The combination Si_3N_4/GaAs is a stiffening layer system whose elastic parameters have been measured by standard acoustical methods.[13]

II. SAMPLES

Silicon nitride (Si_3N_4) exists in various forms, and its exceptional properties make it attractive for many applica-

tions. As a hot pressed ceramic it displays high-mechanical strength and fracture toughness at room and elevated temperatures, which lends this material to uses such as cantilevers in atomic force microscopy. In its amorphous form, silicon nitride has found application in integrated circuits and as insulated layers in thin film transistors and in solar cell applications. Its uses also extend to sensors and photodetectors, which exploit its chemical inertness.

The Si_3N_4 film in our experiments was obtained from Motorola Inc.[14] It was grown by the low-temperature plasma-enhanced chemical-vapor deposition technique on the (001) surface of a GaAs single-crystal wafer. With the growth conditions being temperature 250 °C, pressure 0.9 torr, and RF power 25 W, the growth rate was about 11 nm/mm. These deposition conditions are similar to those used in semiconductor circuit fabrication. Such films are known for their deviation from the stoichiometry implied by Si_3N_4 because of the significant amount of hydrogen incorporated into the film. These films tend to be silicon rich, having a Si N ratio of about 9:10 and they are even more silicon rich at the initiation of the film growth. For the film we investigated, a thickness of 497 nm was measured by profilometry and optical methods, and the density of 2500 kgm^{-3} was obtained by weighing the sample before and after deposition of the film.[14]

Previous studies performed on bulk silicon nitride have attributed variation of the elastic moduli to changes in the density of the material, when in the form of hot pressed and slip-cast ceramics. In the past, silicon nitride films have been studied mostly from a structural and optical point of view. Measurements of the elastic properties have been performed by Hickernell *et al.*[14,13] for silicon nitride deposited on GaAs (001), in layer thicknesses ranging from 200 to 1000 nm. The 497 nm thick sample used in those studies is the specimen we have used in the present study. Hickernell *et al.* measured SAW propagation with an IDT transducer, and by varying the wavelength of the transducer they were able to determine the elastic constants C_{11} and C_{44} of the films. This technique requires the photolithographic patterning of linear arrays of thin-film aluminum interdigital electrodes on top of the film.

III. EXPERIMENTAL TECHNIQUE

A detailed description of the Brillouin scattering experimental set-up has been published elsewhere.[15] In brief, light from an argon ion laser ($\lambda_0 = 514.5$ nm and beam power of 60 mW) was focused onto the film with a $f/5.6$ lens ($f = 50$ mm). The scattered light was collected with the same lens in a backscattering geometry and analyzed using a high contrast and high-resolution Brillouin spectrometer, which incorporated a tandem six-pass Fabry-Perot interferometer.[16] The light was detected by a single-photon counting module and its output was stored in a multichannel scaler card for further analysis. Each spectrum was accumulated for 1–2 hours. The frequencies corresponding to each of the peaks were determined by a curve-fitting routine.

IV. THEORY

We treat here the inelastic scattering of light from an opaque semi-infinite elastically anisotropic solid occupying the half space $x_3 > 0$ and covered with a thin transparent anisotropic film of thickness h, occupying the region $-h < x_3 < 0$ (Fig. 1). We invoke the ripple mechanism, which assumes the scattering is mediated by thermally induced dynamic corrugations in the interface and to a lesser extent in the free surface of the film. There is also elasto-optic scattering in the film and substrate and interference between the different channels that take place, but we have not included these effects in our computations, since they mainly influence the intensity of the Brillouin peaks rather than their positions, which are our prime concern.

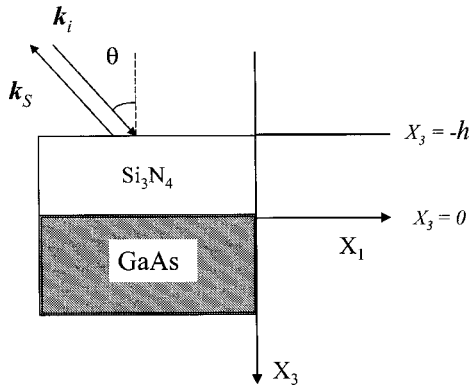

FIG. 1. Backscattering geometry.

At room temperature and above, the cross-section for ripple scattering at either surface is given by[17]

$$\frac{d^2\sigma}{d\Omega_S d\omega_S} = \frac{AT}{\omega} \mathrm{Im}\{G_{33}(\mathbf{k}_\parallel, x_3, \omega + i0)\}, \tag{1}$$

where T is the absolute temperature, $\omega = \omega_I - \omega_S$, where ω_I is the frequency of the incident light, and ω_S is the frequency of the scattered light, A is a constant for a particular surface, which depends on the optical properties of the adjacent media, the scattering geometry and light polarization, $\mathbf{k}_\parallel = (k_1, k_2) = \mathbf{k}_\parallel^I - \mathbf{k}_\parallel^S$ is the projection on the surface of the light-scattering wave vector, and $G_{33}(\mathbf{k}_\parallel, x_3, \omega)$ is the Fourier coefficient of the dynamical Green's tensor pertaining to force and displacement response normal to the surface.[18–20] The location x_3 of the surface takes on the value 0 for scattering from the interface and $-h$ for scattering from the free surface of the film. In the back-scattering geometry of our experiments the wave-vector component $\mathbf{k}_\parallel$ is determined by the angle of incidence, θ, between the normal to the surface and incident light direction, as shown in Fig. 8, and wavelength of the incident light λ_0:

$$|\mathbf{k}_\parallel| = \frac{4\pi \sin\theta}{\lambda_0}. \tag{2}$$

For details of how $G_{33}(\mathbf{k}_\parallel, x_3, \omega)$ is calculated we refer to Ref. 21. The method takes into account the six partial waves ($n = 1,2,...,6$) in the film and the 3 outgoing partial waves ($n = 7,8,9$) in the substrate. These waves for each medium are obtained as solutions of the Christoffel equations

$$(C_{ijkl}k_jk_l-\rho\omega^2\delta_{il})U_l=0, \tag{3}$$

where ρ is the mass density and C_{ijkl} is the elastic modulus tensor of the medium, and U_l are the components of the mode polarization vector. Phase matching of the partial waves in the interface fixes the value of $\mathbf{k}_\parallel$, and ω, and the characteristic equation of Eq. (3) yields six real or complex solutions for k_3. For the substrate, the three incoming waves, characterized by energy flow towards the surface, or exponential growth away from the surface are discarded, and remaining three waves retained. The boundary conditions for the surface and interface tractions, and of continuity of displacement field at the interface yield nine equations for the partial wave amplitudes. The displacement Green's function $G_{33}(\mathbf{k}_\parallel,x_3,\omega)$ is then represented by the superposition of the six partial waves in the film, i.e.,

$$G_{33}(\mathbf{k}_\parallel,x_3,\omega)=\sum_{n=1}^{6}\frac{i}{\omega}(\mathbf{B}^{-1})_p^{(n)}U_3^{(n)}\exp^{ik_3^{(n)}x_3}, \tag{4}$$

where $\mathbf{B}^{-1}$ is the boundary condition matrix, $p=3$ for the surface and 6 for the interface Green's function.

We point out that there is another approach that can be used in calculating Brillouin spectra of supported films.[22,23] This is based on the determination of the displacement field as a superposition of the normal modes for given $\mathbf{k}_\parallel$, taking account of boundary conditions. From comparison we have made with published results, the two approaches appear to be equivalent.

The dispersion or velocity variation of the SAW propagating on a thin film is a function of qh, the product of the absolute value of $\mathbf{k}_\parallel$ and the film thickness h. One can distinguish between two principal domains of behavior, depending on the relative properties of the film and substrate. When the bulk shear wave velocity of the film is lower than that of the substrate, the film loads the substrate and, with increasing h, the SAW velocity decreases and asymptotically approaches the SAW velocity of the film material. In addition, at certain critical values of qh, higher order SAW called Sezawa modes and longitudinal guided modes emerge from the bulk wave continuum.[1]

On the other hand, if as is the case considered here, the shear velocity of the film is larger than that of the substrate (stiffening case), the SAW velocity initially grows with increasing qh. At a critical value qh_{cut} the SAW meets and degenerates with the bulk wave continuum. The threshold slowness (inverse phase velocity) at which this occurs is called the transonic state.[1] Beyond this cutoff, while no true SAW any longer exists, there is a pseudo surface acoustic wave (PSAW), which radiates energy into the substrate and as a result attenuates with distance as it travels along the surface. The attenuation reaches a maximum slightly beyond qh_{cut} and then subsides, either tending towards zero or leveling off at a finite value, depending on the conditions.[9] Recent calculations of the dispersion of SAW above cutoff in stiffening systems[10] have revealed two types of PSAW dispersion. The first type of behavior comes about when the elastic properties of the layer and the substrate are not very different, and has the velocity of the pseudosurface wave beyond cut off increasing up to the Rayleigh wave velocity

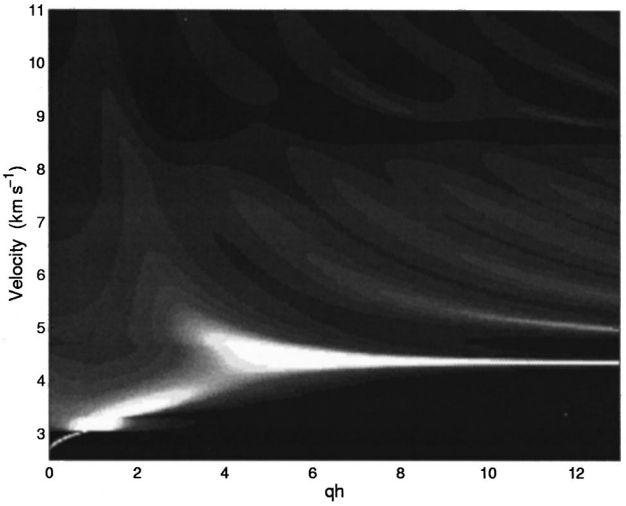

FIG. 2. Two-dimensional gray image of the calculated Brillouin spectra of Si_3N_4/GaAs at free Si_3N_4 surface.

of the layer, while the attenuation of this wave tends asymptotically to zero. We will call this type of behavior the nonsplitting type. The second type of behavior arises when the elastic properties of the two materials are quite dissimilar, and has the PSAW evolving into a strongly attenuated interfacial mode, while a second mode appears at a higher velocity, and evolves into the Rayleigh wave at the free surface of the layer. We will call this second type of behavior of the dispersion relation the splitting type. The nonsplitting type of behavior has been observed experimentally in an alumina film on aluminum[9] and in a titanium nitride film on steel.[4] The Si_3N_4 film on GaAs substrate in our present experiments is a stiffening system since V_{hear} of the Si_3N_4 and GaAs are[25] -4700 m/s and -3300 m/s respectively, and we will demonstrate now that the SAW dispersion is of the splitting type. In experiments we measured only one branch of the dispersion curve corresponding to SAW's propagating in the [100] direction on the (001) GaAs surface. The Si_3N_4 film is assumed to be isotropic.[14]

Gray scale images representing the calculated Brillouin intensity as a function of velocity $V=\omega/k_\parallel$ and qh, for scattering from the free surface of the film and from the interface between the film and substrate for the [100] direction in the (001) surface of GaAs are presented in Figs. 2 and 3, respectively. The gray scale intensity in these images is proportional to $\omega^{-1}\,\text{m}\{G_{33}(\mathbf{k}_\parallel,x_3,\omega+i0)\}$, with $x_3=0$ for the interface and $x_3=-h$ for the surface of the film. In our calculations we have used the elastic constants obtained by Hickernell *et al.*[14] for isotropic polycrystalline Si_3N_4: $C_{11}=189$ and $C_{44}=56$ GPa and the following published values of the elastic constants for cubic GaAs:[26] $C_{11}=118.1$, $C_{12}=53.2$, and $C_{44}=59.4$ GPa. Brillouin spectra calculated for $qh=0.5$, 2, and 8, with scattering taking place at the surface are shown in Fig. 4. For $qh=0$, the velocity corresponds to the SAW velocity on the GaAs substrate. With increasing qh the SAW velocity approaches the bulk wave threshold or limiting shear slowness $\mathbf{k}_\parallel/\omega$, which is reached at $qh_{\text{cut}}\approx 1.5$. Below qh_{cut} the Brillouin spectrum displays a sharp peak, which is associated with the true surface wave and in addition a continuum extending from the bulk wave thresh-

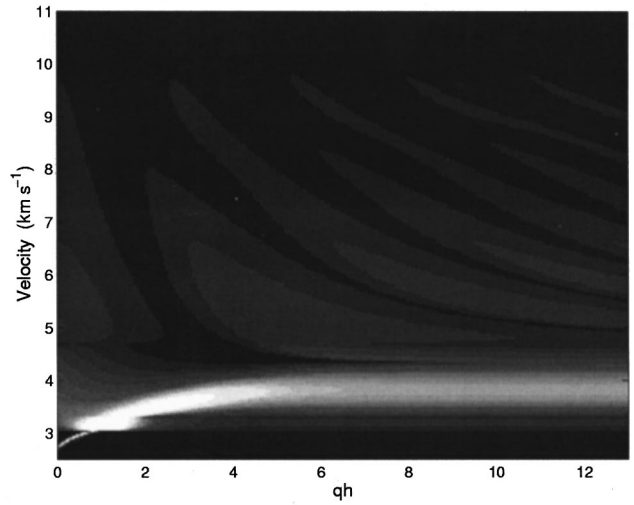

FIG. 3. Two-dimensional gray image of the calculated Brillouin spectrum at Si_3N_4/GaAs interface.

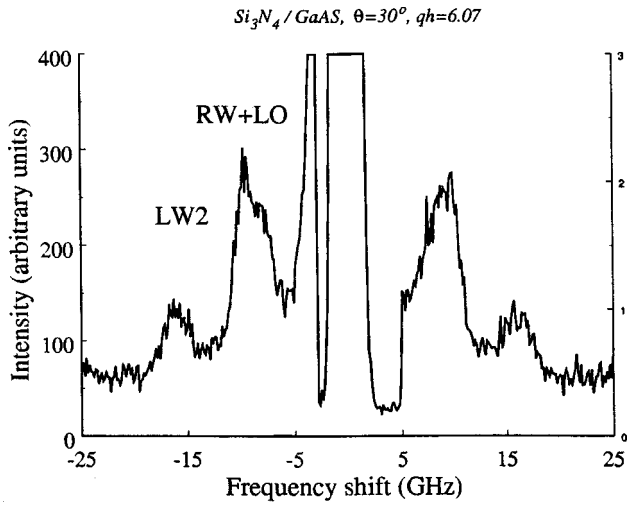

FIG. 5. Brillouin experimental spectrum of Si_3N_4 film for the angle θ of 30°.

old to higher frequencies, which is known as the Lamb shoulder. In our calculation of the Green function (1) a small amount of artificial damping[27] is introduced to avoid a true singularity. In the region below cutoff, the position of the SAW peak is the same for surface and interface scattering. This range of small $qh<1.5$ has been experimentally investigated by Hickernell *et al.*[13,14] At qh_{cut}, the SAW degenerates with the bulk continuum, and beyond cutoff there is no true SAW. In its place there are broadened resonances, which are associated with attenuated PSAW at the interface or surface of the film, and that leak energy into the substrate. Somewhat above the cut-off velocity, the Brillouin spectrum for the interface displays a broad peak which beyond $qh \approx 4$ becomes independent of the film thickness. This peak is associated with a highly damped interfacial wave. Its broadening is due to leakage of energy into the substrate as discussed in Ref. 10. In the same spectral region, the calculated Brillouin spectrum for the surface of the film displays a broad peak, which fades away by $qh \approx 4$. At this point another broad peak appears, which with increasing qh becomes narrower, as the associated mode tends towards the Rayleigh mode of Si_8N_4 (see graph for $qh=8$ on Fig. 4). For very large qh this becomes the true nondispersive Rayleigh SAW.

With increasing qh, a succession of higher order damped Lamb modes come into view in Fig. 2, moving downwards in velocity and eventually leveling off, but remaining damped.

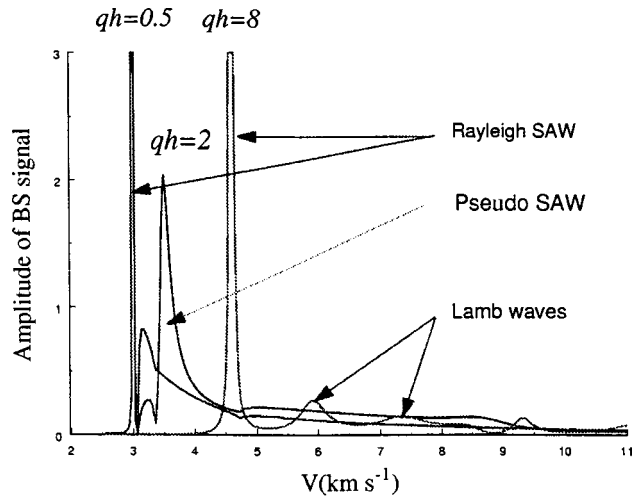

FIG. 4. Calculated Brillouin spectra of Si_3N_4/GaAs for a section of film thickness h, displaying Rayleigh SAW, a highly damped PSAW, and Rayleigh wave on the film and higher order Lamb modes. The scattering intensity is given in arbitrary units.

V. RESULTS AND DISCUSSION

The typical Brillouin spectra of the Si_3N_4 film that we have recorded are shown in Figs. 5–8. Four distinct spectral components are observed approximately symmetrically positioned on either side of the central elastic peak. The upshifted (anti-Stokes) components are due to phonon annihilation, and the downshifted (Stokes) components are due to phonon creation. For the purpose of our discussion, the five components starting from the one closest to the central peak are labeled *IW*, *RW*, *LO*, *LW*1, and *LW*2. To make peaks around main maxima (*RW*) more discernible we repeated measurements of SBS spectrum for five times. Averaged SBS spectra measured at 60° and 65° are presented in Figs. 6 and 8 (bottom). To separate the *IW*, *RW*, *LO* modes (Fig. 7) we used multipeaks (Lorentzian) fitting subrotune within software package called Origin from Microcal Software, Inc., Northampton, MA built-in Origin (Microcal).

We have recorded Brillouin spectra for scattering angles θ ranging from 20° to 70° in steps of 5°. On the assumption that the peaks are due to surface phonons, their corresponding velocities are given by

$$V_{\mathrm{SAW}}=\frac{f\cdot\lambda_0}{2\sin\theta}, \tag{5}$$

where, V_{SAW} is the SAW velocity and f is the frequency shift

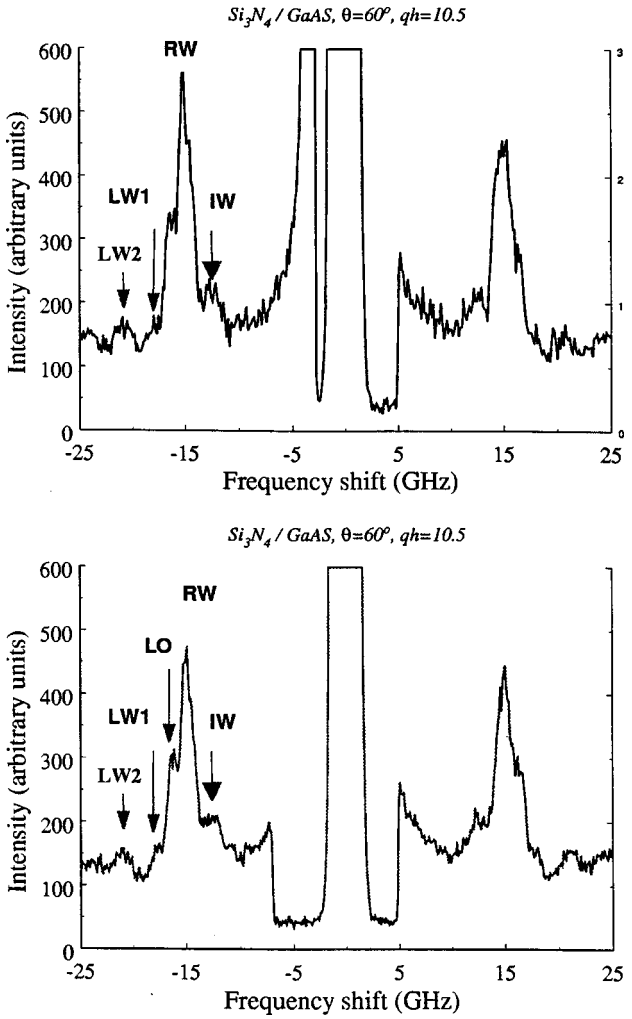

FIG. 6. Brillouin experimental spectrum of Si_3N_4 film for the angle θ of 60°. Top. Single spectrum accomulated for 2 h. Spectrum obtained by averaging over five spectra accomulated for 1 h.

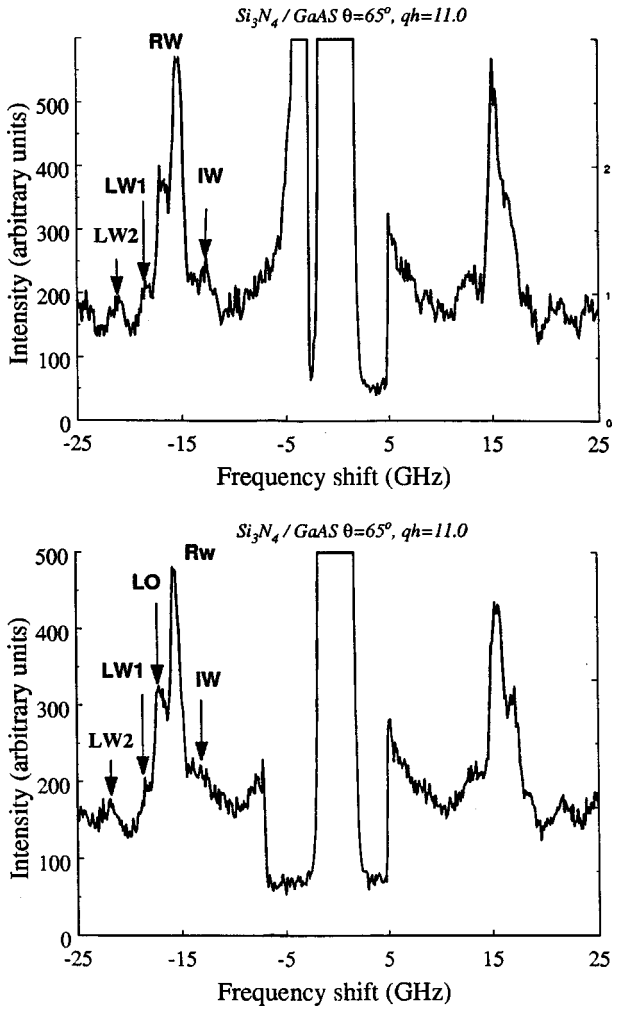

FIG. 8. Brillouin experimental spectrum of Si_3N_4 film for the angle θ of 65°. Top. Single spectrum accomulated for 2 h. Bottom. Spectrum obtained by averaging over five spectra accomulated for 1 h.

of the spectral feature. The measured surface wave velocities as a function of qh are plotted in Fig. 9. The data presented cover the range $qh=4$ to $qh=12$. We are able to identify the Rayleigh surface mode and second-order damped Lamb

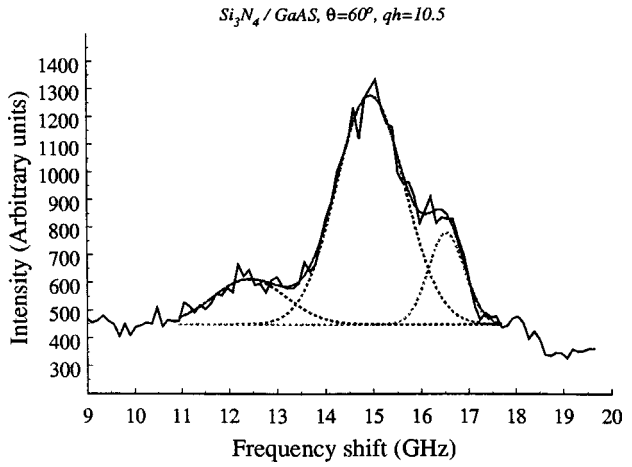

FIG. 7. Brillouin experimental spectrum of Si_3N_4 film for the angle θ of 60°. Fitting of *LO*, Rayleigh, and *IW* modes by Lorenzian-shaped peacks.

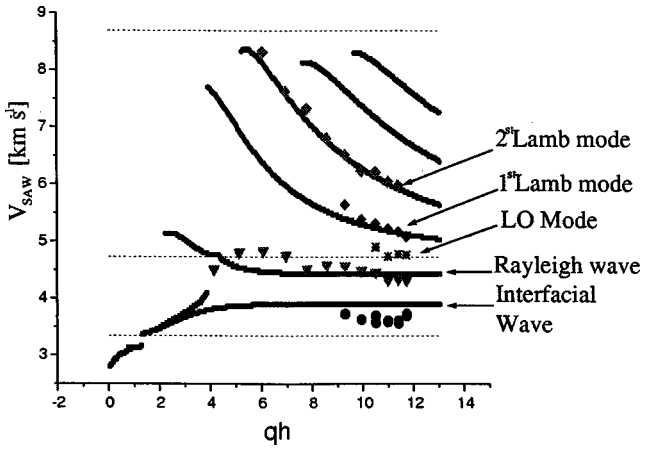

FIG. 9. Dispersion curves calculated using Green function and experimental results of Si_3N_4/GaAs. Dashed lines are shear cutoff (lower line), longitudinal cutoff (middle line) in the [100] direction on the (001) GaAs surface and longitudinal cutoff for Si_3N_4 (upper line).

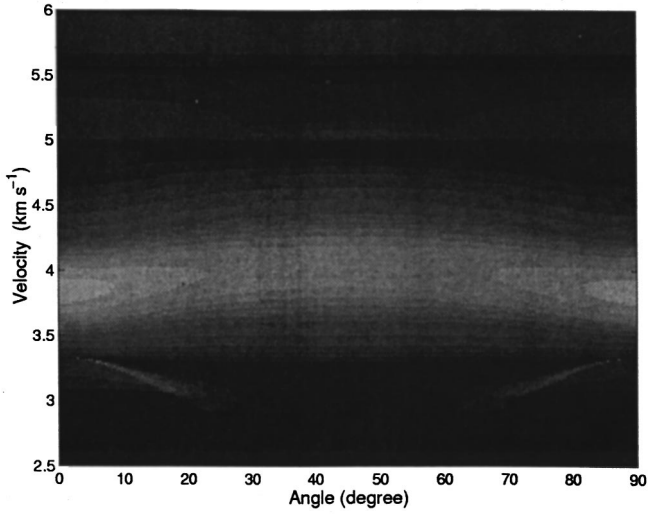

FIG. 10. Brillouin spectrum calculated for the interface as a function of the rotation angle.

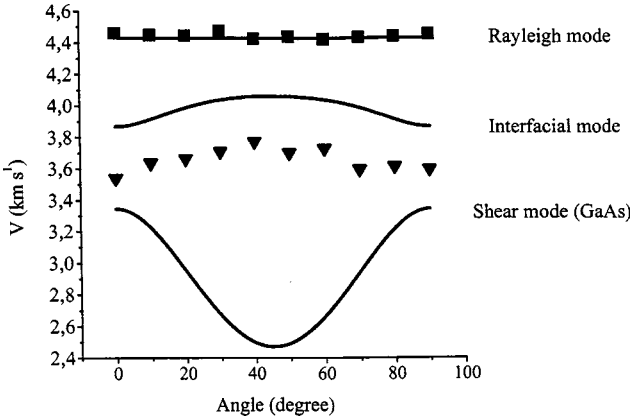

FIG. 11. Angle dependence of the Rayleigh, interfacial, and shear mode in GaAs. Theoretical points for Rayleigh (solids rectangles) and interfacial modes (solid triangles) were taken from Brillouin spectra measured for $qh=11$ (angle of incident light to surface normal is equal to 60°).

mode for the entire range of *qh*. The first Lamb mode can only be identified for angles greater than 50°.

The dispersion curves in Fig. 9 represent the traces of the maxima of the calculated Brillouin intensity (Fig. 3) for the interface (the lowest solid line) and surface (Fig. 2, the upper solid lines) and of the measured Brillouin intensity. The experimental data are in excellent agreement with the theoretical predictions for all except the interfacial mode and the fact of the disappearance of the first Lamb mode in the measured spectrum at small *qh*. The former discrepancy suggests that the interface is more complicated than assumed in our model. There could well be a compositional variation extending over some tens of nanometers, as has been reported for the TiN-steel interface by Refs. 28 and 20. For thin films this compositional variation also has a pronounced effect on the scattering from the surface of the film. Indeed, there have been numerous reports on films of thickness less than 100 nanometers, for which the Brillouin measured Rayleigh velocities are significantly less than predicted on the basis of bulk values of the elastic constants.[29,30,28,20] We note that similar behavior of the Rayleigh branch has been observed in a film of CaF_2 film on GaAs (111).[31] However, the dispersion relation for SAW on CaF_2/GaAs (111) is not of the splitting type. Calculations of the interfacial Green's function for that system reveal no interfacial mode.

The other discrepancy that needs to be accounted for is that the intensity of the first Lamb mode is too weak to be detected in the angular range 20° to 45°. To accurately account for the positions as well as intensities of the peaks in the Brillouin spectrum of a solid covered by a transparent film,[32] one needs to consider not only ripple scattering from the surface and interface, but also elasto-optic scattering in the film and substrate and interference between these channels. Under certain conditions, interference can have the effect of almost completely suppressing a Brillouin peak. While we have not included these effects in our computations, a simple estimate based on the optical path lengths in the Si_3N_4 film lead to the conclusion that the first Lamb peak should be considerably suppressed in comparison with the higher Lamb modes. For the first Lamb mode this phenomena was predicted by Bortolani *et al.*[32] and observed in Refs. 23, 33, and 24.

To test the anisotropic properties of the interfacial wave, the scattering angle θ was fixed at 60° and the film was rotated about the normal to the film's surface in steps of 10°, and for each orientation, a Brillouin spectrum was recorded. A theoretical gray scale image and experimentally measured results are presented in Figs. 10 and 11, respectively. Variation of the velocity of the interfacial wave with angle is around 5%. Experimental data reproduce the shape of theoretical curve, but the measured and calculated velocity curves are offset by 0.25 km s^{-1}. It is interesting to note that the variation of the velocity of the shear wave in GaAs is completely different in character to the interfacial wave. Little variation (less than 1%) is observed in the velocity of the Rayleigh wave.

LO peak is well distinguished on the SBS spectra in the angular range 60° to 70° (Figs. 6, 7, and 8). It can be attributed to longitudinal leaky wave propagating in GaAs along Si_3N_4/GaAs interface. Similar peak detected in SBS spectrum of GaAs surface has been explained by Bortolany *et al.*[34] as due to leaky longitudinal surface mode and the elasto-optic coupling. At the beginning of the dispersion curves ($kh \lesssim 10$) where the main peak $LO+RW$ (Fig. 5) is broad, *LO* and *RW* modes are difficult to resolve.

VI. CONCLUSIONS

(1) A splitting in the dispersion curve of SAW's in thin film Si_3N_4 on GaAs has been observed by surface Brillouin spectroscopy. Existence of the two branches of the dispersion curve (Rayleigh and pseudointerfacial modes) above cut-off predicted theoretically[10] has thus been confirmed. This is the first reported observation, for a stiffening layer on a substrate, of a leaky interfacial wave, a type of mode that is of potential value in the interface characterization of thin supported transparent films.

(2) The measured velocity of the interfacial wave is

smaller than predicted on the basis of the bulk elastic constants of the media, and this is indicative of compositional variation in the vicinity of the interface

(3) The other peaks in the Brillouin spectrum are associated with modes which sample the elastic properties of the entire film, and are not influenced to the same degree by the interfacial region. For these peaks, the calculated and measured frequency shifts are in good agreement. To better account for the intensities of these peaks, elasto-optic scattering and interference effects would need to be taken into account.

ACKNOWLEDGMENTS

The support for the facilities was provided by the W. M. Keck Foundation and the National Science Foundation (Grant No. 8720404). We are grateful to T. S. Hickernell for providing the sample, T. Kundu for helpful suggestions, and J. Balogh and 0. Matthews for technical assistance.

[1] G. W. Farnell and E. L. Adler, in *Physical Acoustics*, edited by W. P. Mason and R. N. Thurston (Academic, New York, 1972), Vol. IX, p. 35.

[2] L. M. Brekhovskikh, *Waves in Layered Media*, 2nd ed. (Academic, New York, 1980).

[3] H. Holleck, J. Vac. Sci. Technol. A **4**, 2661 (1986).

[4] W. Pang, P. R. Stoddart, J. D. Comins, A. G. Every, D. Pietersen, and P. J. Marais, Int. J. Refract. Met. Hard Mater. **15**, 179 (1997).

[5] D. Schneider, T. Schwarz, and B. Schultrich, Thin Solid Films **219**, 92 (1992).

[6] D. Schneider, T. Schwarz, H. J. Scheibe, and M. Panzner, Thin Solid Films **295**, 107 (1997).

[7] P. Hess, Appl. Surf. Sci. **106**, 429 (1996).

[8] D. B. Bogy and S. M. Gracewski, J. Acoust. Soc. Am. **74**, 591 (1983).

[9] P. Zinin, O. Lefeuvre, G. A. D. Briggs, B. D. Zeller, P. Cawley, A. J. Kinloch, and G. E. Thompson, J. Appl. Phys. **82**, 1031 (1997).

[10] O. Lefeuvre, P. Zinin, G. A. D. Briggs, and A. Every, Appl. Phys. Lett. **72**, 856 (1998).

[11] E. Palik, *Handbook of Optical Constants of Solids* (Academic, Orlando, 1985).

[12] O. B. Wright, Opt. Lett. **20**, 632 (1995).

[13] F. S. Hickernell and T. S. Hickernell, IEEE Trans. Ultrason. Ferroelectr. Freq. Control **42**, 410 (1995).

[14] T. S. Hickernell, F. M. Fliegel, and F. S. Hickernell, in *Proceedings IEEE 1990 Ultrasonics Symposium*, edited by B. R. McAvoy (Institute of Electrical and Electronics Engineers, New York, 1990), p. 445.

[15] V. Askarpour, M. H. Manghnani, S. Fassbender, and A. Yoneda, Phys. Chem. Miner. **19**, 511 (1993).

[16] J. R. Sandercock, in *Light Scattering in Solids III. Recent Results*, edited by M. Cardona and G. Guntherodt Topics in Applied Physics Vol. 51 (Springer-Verlag, Berlin, 1982), p. 173.

[17] M. G. Cottam and A. A. Maradudin, in *Surface Excitations*, edited by V. M. Agranovich and R. Loudon (Elsevier, London, 1984), p. 5.

[18] R. Loudon, Phys. Rev. Lett. **40**, 581 (1978).

[19] K. R. Subbaswamy and A. A. Maradudin, Phys. Rev. B **18**, 4181 (1978).

[20] A. G. Every, W. Pang, J. D. Comins, and P. R. Stoddart, Ultrasonics **36**, 223 (1998).

[21] X. Zhang, J. D. Commins, A. G. Every, P. R. Stoddart, W. Pang, and T. E. Derry, Phys. Rev. B **58**, 13 667 (1998).

[22] V. Bortolani, A. Franchini, F. Nizzoli, G. Santoro, G. Benedek, and V. Celli, Surf. Sci. **128**, 249 (1983).

[23] V. Bortolani, F. Nizzoli, G. Santoro, and J. R. Sandercock, Phys. Rev. B **25**, 3442 (1982).

[24] L. Sun, J. R. Dutcher, L. Giovannini, F. Nizzoli, J. R. Stevens, and J. L. Ord, J. Appl. Phys. **75**, 7482 (1994).

[25] A. J. Slobodnik, E. D. Conway, and R. T. Delmonico, *Microwave Acoustics Handbook* (Air Force Cambridge Research Laboratories, Cambridge, 1973).

[26] A. G. Every and A. K. McCurdy, in *Numerical Data and Functional Relationships in Science and Technology*, edited by O. Madelung, Landoldt-Börnstein, New Series, Group III, Vol. 29, Pt. a (Springer, Berlin, 1992).

[27] A. G. Every, K. Y. Kim, and A. A. Maznev, J. Acoust. Soc. Am. **102**, 1 (1997).

[28] W. Pang, Ph.D. thesis, University of the Witwatersrand, 1998.

[29] B. Hillebrands, P. Baumgart, R. Mock, G. Guntherodt, and P. S. Bechthold, J. Appl. Phys. **58**, 3166 (1985).

[30] G. Carlotti, D. Fioretto, L. Palmieri, G. Socino, L. Verdini, and E. Verona, IEEE Trans. Ultrason. Ferroelectr. Freq. Control **38**, 56 (1991).

[31] V. V. Aleksandrov, C. E. Bottani, G. Caglioti, G. Ghislotti, C. Marinoni, P. Mutti, N. L. Yakovlev, and N. S. Sokolov, J. Phys.: Condens. Matter **6**, 1947 (1994).

[32] V. Bortolani, A. M. Marvin, F. Nizzoli, and G. Santoro, J. Phys. C **16**, 1757 (1983).

[33] J. M. Karanikas, R. Sooryakumar, and J. M. Phillips, Phys. Rev. B **39**, 1388 (1989).

[34] V. Bortolani, F. Nizzoli, and G. Santoro, Phys. Rev. Lett. **41**, 39 (1978).